We are IntechOpen, the world's leading publisher of Open Access books Built by scientists, for scientists

6,900
Open access books available

185,000
International authors and editors

200M
Downloads

Our authors are among the

154
Countries delivered to

TOP 1%
most cited scientists

12.2%
Contributors from top 500 universities



WEB OF SCIENCE™

Selection of our books indexed in the Book Citation Index in Web of Science™ Core Collection (BKCI)

Interested in publishing with us?
Contact book.department@intechopen.com

Numbers displayed above are based on latest data collected.
For more information visit www.intechopen.com



13

Numerical Simulation of Plasma-Chemical Processing Semiconductors

Yurii N. Grigoryev and Aleksey G. Gorobchuk
Institute of Computational Technologies Russian Academy of Sciences, Siberian Branch
Russia

1. Introduction

The growing rates of microchip world production during the last two decades exceed essentially the corresponding indexes of any others production branches. Between 1997 and 2003 the consumer and communication electronics sales have grown from USD 744 billion to about USD 165 trillion. The present-day electronics is based on a silicon technology and such a state will be conserve at least during the nearest ten years. The low temperature plasma facilities - so called plasma reactors or glow discharge reactors, play an important role in technological processes of chip production.

Such reactors are widely used for etching and deposition of semiconductor films, for taking off photoresist and some other operations. Very often they enter the complex cluster equipment for making chips.

Some characteristic schemes of these glow discharge reactors are presented in Fig. 1. The typical reactor consists of two parallel plate electrodes forming an axisymmetrical cylinder chamber, in which the high-frequency discharge is appeared. The processing wafer is placed on one of the electrodes. The originally inert feed gas enters the discharge zone where an active etchant species is produced by the electron - impact dissociation. The active species transfers to the wafer and reacts with it forming the volatile products. The unreacted feed gas and the products of physical-chemical processes and reactions are pumped outwards from the reactor.

From the presented schemes one can see that these reactors are not very complicated and expensive apparatus. But yet in 1995 a world volume of sales of the reactors have made up USD 2 billion and it keeps on growing. This numeral can give us a rough idea about the quantity of operative reactors in modern industry.

Despite of the relative simple construction the etching process in a reactor is a very complicative one. For silicon wafer operating the complex molecular gases such as CF_4, SF_6 and their mixtures with oxygen O_2 and hydrogen H_2 are used. Under a microwave discharge and ion current in etching chamber a reacting medium appears which is characterized by simultaneously proceeding processes of ionization, dissociation, heat and mass transfer with complex chemical reactions. A similar processes take place on the surfaces of the chamber and wafer under operating.

The quality and manufacturing rate of producing chips depend strongly on a large number of process variables in a reactor including parent gas composition, pressure, temperature, frequency and power of a discharge, flow rate and configuration, etc. Because of numerous

Source: Micro Electronic and Mechanical Systems, Book edited by: Kenichi Takahata,
ISBN 978-953-307-027-8, pp. 572, December 2009, INTECH, Croatia, downloaded from SCIYO.COM

and complex interconnections of the factors which defines the qualities of etching wafer, the opportunities of experimental studies and optimization of reactor process are very restricted.

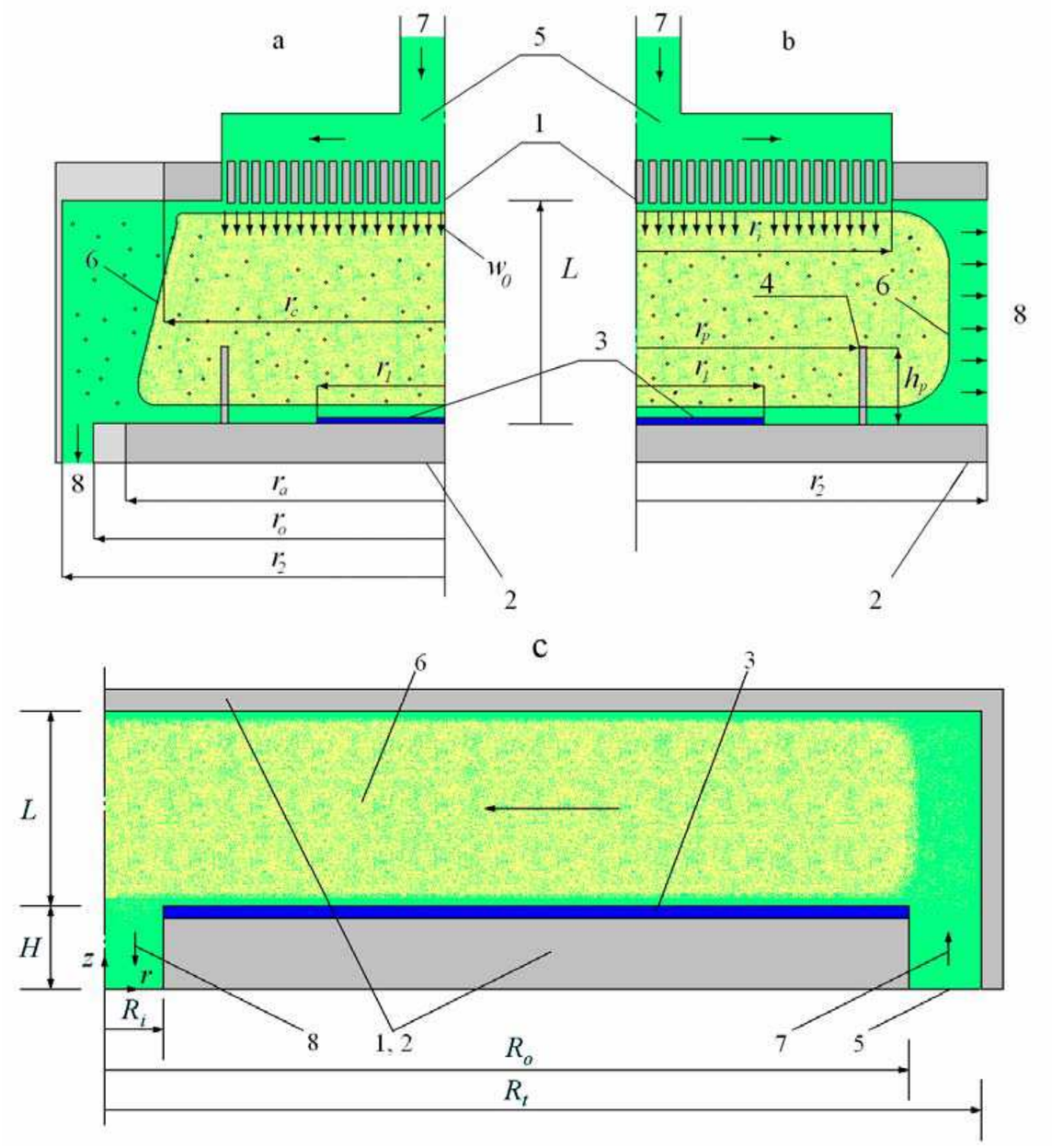


Fig. 1. The schemes of plasma - chemical etching reactors: a – "pedestal", b – "stadium", c - radial flow reactor. 1, 2 - RF - electrodes, 3 - processing wafer, 4 - protector, 5 - feed gas, 6 - RF - discharge zone, 7 - inlet, 8 - outlet. The arrowed lines show the direction of the gas flow in the reactor.

A natural alternative here is the mathematical modelling. It is especially necessary in respect to insufficient understanding of many real plasma physics and chemistry governing mechanisms which take place in this apparatus.

By such a way there are economical, technical and scientific preconditions for the well-directed efforts in the development of mathematical modelling of plasma etching reactors.

2. Numerical model formulation

In first turn some characteristic features of authors' numerical model of plasma etching process will be described. The numerical model was developed during several years with successive improving its adequacy and prognostic abilities step by step (Grigoryev & Gorobchuk, 1996; Grigoryev & Gorobchuk, 1997; Grigoryev & Gorobchuk, 1998; Shokin et al., 1999; Grigoryev & Gorobchuk, 2004; Grigoryev & Gorobchuk, 2007; Grigoryev & Gorobchuk, 2008). Today the created model corresponds completely to the world standards in mathematical modelling of plasma reactors and includes some novel elements.

2.1 Gas flow and temperature distribution

Under the typical operating conditions in plasma reactors the continuum approach is valid, and gas flow is laminar, viscous and incompressible. Therefore, the steady Navier - Stokes equations with heat transfer in standard Boussinesq approximation were used for the flow description (Grigoryev & Gorobchuk, 1997; Grigoryev & Gorobchuk, 1998; Shokin at al., 1999). The axisymmetric statement of a problem is considered. The conservation equation of total mass (continuity equation) was written as follows:

$$\nabla \cdot \mathbf{v} = 0 \tag{1}$$

The conservation equation of momentum had the form:

$$\begin{aligned} \rho_0 \mathbf{v} \cdot \nabla \mathbf{v} &= \nabla \cdot \tau - \rho_0 \mathbf{g} \beta (T - T_0), \\ \tau &= -p\mathbf{I} + \eta[\nabla \mathbf{v} + (\nabla \mathbf{v})^*] \end{aligned} \tag{2}$$

where ρ is a density of gas mixture, $\mathbf{v}$ is a fluid velocity vector, p is a pressure, τ is a stress tensor, $\mathbf{I}$ is a identity matrix, T is a local temperature of gas mixture, T_0 is a temperature of the feed gas at the inlet of the reactor, $\mathbf{g}$ is a gravitational acceleration vector, β is a thermal expansion coefficient, η is a shear viscosity. The density ρ_0 corresponds to the gas temperature T_0. For the velocity components on impenetrable walls the nonslip boundary conditions were used in range of operating pressures p = 0.1 – 1.0 torr and slip conditions for low pressures p = 0.01 – 0.1 torr correspondingly.

The temperature distribution was obtained by solving the energy balance equation with heat transfer at the surfaces of reactors (Grigoryev & Gorobchuk, 1997; Grigoryev & Gorobchuk, 1998; Shokin et al., 1999):

$$\rho c_p (\mathbf{v} \cdot \nabla T) = \nabla \cdot (\lambda \nabla T) - \nabla \cdot \mathbf{q}_r, \tag{3}$$

where c_p is a constant - pressure heat capacity, λ is a gas thermal conductivity, $\mathbf{q}_r$ is a radiation flow rate. The radiation flow $\mathbf{q}_r$ under operating pressures p = 0.1-1.0 torr was calculated in thin optical layer approximation.

The dynamical and energy balance equations were coupled through the temperature dependence of gas viscosity and the buoyancy term. The gas viscosity, thermal conductivity and heat capacity were considered as functions of temperature. The boundary conditions on the temperature expressed a balance of convective flow, heat conduction and radiation heat

flows at the solid walls. At the axis of symmetry the no flux boundary condition was used. The gas temperature at the inlet of reactor is equal to the wall temperature. Under low pressures a "temperature jump" condition was used.

2.2 Physical-chemical kinetics and species concentration distribution

In general case a binary mixture CF_4/O_2 was considered as a parent gas because it is widely spread in silicon technology (Grigoryev & Gorobchuk, 2004; Grigoryev & Gorobchuk, 2007). An important difficulty for CF_4/O_2 system is a simulation of plasma-chemical kinetics which is extraordinarily complicated. Generally the governing set of chemical reactions and corresponding number of reagents essential for given chemical system are chosen using real experimental data. For Si - CF_4/O_2 parent system a subset of 14 gas-phase reactions were derived which describes adequately the experimental observations (Plumb & Ryan, 1986). This improved chemical kinetic model was added by several heterogeneous reactions with CF_2, CF_3 radicals (Venkatesan at al., 1990; Sang-Kyu Park & Economou, 1991).

The kinetic model included the following processes: electron-impact dissociation of binary gas mixture, volume recombination of reactive atoms and radicals, silicon etching, chemisorption of fluorine and oxygen atoms on Si surface, recombination and adsorption of CF_2, CF_3 at wafer. The complete set of reactions used in the paper looks as follows:

$$CF_4 + e^- \rightarrow^{k_{e1}} CF_3 + F + e^-, \quad (4)$$

$$CF_4 + e^- \rightarrow^{k_{e2}} CF_2 + 2F + e^-, \quad (5)$$

$$O_2 + e^- \rightarrow^{k_{e3}} O + O + e^-, \quad (6)$$

$$COF_2 + e^- \rightarrow^{k_{e4}} COF + F + e^-, \quad (7)$$

$$CO_2 + e^- \rightarrow^{k_{e5}} CO + O + e^-, \quad (8)$$

$$CF_3 + CF_3 + M \rightarrow^{k_{v1}} C_2F_6 + M, \quad (9)$$

$$F + CF_3 + M \rightarrow^{k_{v2}} CF_4 + M, \quad (10)$$

$$F + CF_2 + M \rightarrow^{k_{v3}} CF_3 + M, \quad (11)$$

$$O + CF_3 \rightarrow^{k_{v4}} COF_2 + F, \quad (12)$$

$$O + CF_2 \rightarrow^{k_{v5}} COF + F, \quad (13)$$

$$O + CF_2 \rightarrow^{k_{v6}} CO + 2F, \quad (14)$$

$$O + COF \rightarrow^{k_{v7}} CO_2 + F, \quad (15)$$

$$F + COF + M \rightarrow^{k_{v8}} COF_2 + M, \quad (16)$$

$$F + CO + M \rightarrow^{k_{v9}} COF + M, \quad (17)$$

$$F + F + M \rightarrow^{k_{v10}} F_2 + M, \quad (18)$$

$$F_2 + M \rightarrow^{k_{v11}} F + F + M, \quad (19)$$

$$CF_3 \rightarrow^{k_{s1}} CF_3\,(s), \quad (20)$$

$$CF_2 \rightarrow^{k_{s2}} CF_2\,(s), \quad (21)$$

$$F + CF_2\,(s) \rightarrow^{k_{s3}} CF_3, \quad (22)$$

$$F + CF_3\,(s) \rightarrow^{k_{s4}} CF_4, \quad (23)$$

$$CF_3 + CF_3\,(s) \rightarrow^{k_{s5}} C_2F_6, \quad (24)$$

$$CF_2\,(s) + O \rightarrow^{k_{s6}} CO + 2F, \quad (25)$$

$$CF_3\,(s) + O \rightarrow^{k_{s7}} CO + 3F, \quad (26)$$

$$O \rightarrow^{k_{s8}} O\,(s), \quad (27)$$

$$O\,(s) + F \rightarrow^{k_{s9}} O + F, \quad (28)$$

$$4F + Si \rightarrow^{k_s} SiF_4 \uparrow, \quad (29)$$

$$4F + Si + I^+ \rightarrow^{k_i} SiF_4 \uparrow. \quad (30)$$

where k_{e1}-k_{e5} are the rate constants of electron-impact dissociation of parent gas; k_{v1}-k_{v11} are the rate constants of volume recombination; k_{s1}-k_{s7} are the rate constants of heterogeneous reactions. The designation (s) marks the species adsorbed on the wafer surface. The values of these constants were taken from (Plumb & Ryan, 1986; Venkatesan at al., 1990; Sang-Kyu Park & Economou, 1991).

The model contains 16 gas-phase reactions and 8 heterogeneous reactions on the wafer. Reactions Eqs. (4)-(8) represent the electron-impact dissociation of binary gas mixture; Eqs. (9)-(19) are the reactions of volume recombination of reactive atoms and radicals; Eqs. (20)-(26) are the reactions of recombination and adsorption of CF_2, CF_3 at wafer; Eqs. (27), (28) are the chemisorption processes of fluorine and oxygen atoms on Si surface; Eqs. (29), (30) are the reactions of spontaneous and ion-induced silicon etching correspondingly. The

twelve products of dissociation and recombination processes - F, F_2, CF_2, CF_3, CF_4, C_2F_6, O, O_2, CO, CO_2, COF, COF_2 are taken into account.
Accordingly to multicomponent chemical kinetic model the distribution of species concentration for each component was derived from the system of convective-diffusion equations:

$$\mathbf{v} \cdot \nabla C_i = \nabla \cdot (C_t D_i (\nabla x_i + k_T \nabla \ln T)) + G_i(C_i, C_j), \quad i, j = 1, \ldots, 12, \tag{31}$$

where C_i, x_i are the molar concentration and molar fraction of species i correspondingly, C_t is the molar gas concentration, D_i is the multicomponent diffusion coefficient of species i, k_T is the thermal diffusion relation, G_i is the rate of formation of species i in gas-phase reactions. The gas phase reactions are incorporated in right-hand side of this system and define a complex interconnection between all species generation processes. The surface and silicon etching reactions entered the boundary conditions at the wafer. The latter were written as a balance of mass flows for each component. At the reactor inlet the Danckwert's type boundary conditions were stated (Sang-Kyu Park & Economou, 1991). The feed species concentrations at the inlet are fixed. No radial gradients of species concentrations are considered at the reactor centerline. At the reactor outlet, zero axial gradients of species concentrations are also used.

2.3 Glow discharge structure and electron concentration

The exact calculation of glow discharge structure demands a solving the Boltzmann kinetic equation for the electrons in a mixture multiatomic gases and radicals. From both physical and computational points of view this is a formidable task (Aydil at al., 1993). Therefore in the parametric calculations some simplest model distributions of electron density in reactor were used. Depending on the pressure and gas medium under consideration, the dominant electron loss mechanism can be diffusion, recombination or attachment. In calculations usually it was assumed that the electron density distribution corresponded to a “diffusion-dominated” discharge (Dalvie at al. 1986).

2.4 Numerical method

The presence of two-order elliptic operators in all equations of the mathematical model allows us to approximate each equation by implicit iterative finite difference splitting-up scheme with stabilizing correction (Grigoryev & Gorobchuk, 1996). The scheme in general form looks as follows:

$$\frac{\phi^{k+1/2} - \phi^k}{\tau} = L_r^{\phi} \phi^{k+1} + L_z^{\phi} \phi^k + F(\phi^k),$$
$$\frac{\phi^{k+1} - \phi^{k+1/2}}{\tau} = L_z^{\phi} (\phi^{k+1} - \phi^k).$$

The scheme has $O(\tau + h_1^2 + h_2^2)$ approximation order where h_1, h_2 are the mesh sizes along r and z coordinates, τ is the iterative parameter. The solution of the original steady state problem was derived by the relaxation method. The iterative process was terminated after achieving the relative error $\varepsilon_{\phi} = 10^{-10} - 10^{-4}$ in the uniform norm

$$\max_{\Omega_h} \left| \frac{\phi^{k+1} - \phi^k}{\tau \phi^{k+1}} \right| < \varepsilon_\phi .$$

The equations (1), (2) were solved together with the heat transport equation (3). Calculations were worked out in the "stream function – vorticity" variables. The second-order Thom's vorticity boundary condition was applied to the flow problem. The stream function and gas temperature were found for each iteration of vorticity. The species concentrations were then calculated from the convective - diffusion equations (31) using the resulting velocity and temperature distributions.

3. Main results of plasma-chemical reactor modelling

Here some new effects obtained in our studies will be commented. These effects were not considered before in the literature.

3.1 Optimization of reactor design with respect to etching uniformity

Firstly it will be demonstrated that the mathematical modelling even in frameworks of simplified model can give the results useful for technical applications. In (Grigoryev & Gorobchuk, 1996) we considered two most spread plasma-chemical etching reactor schemes - "pedestal" and "stadium" ones, which are used for individual etching of wafer with diameters up to 500 mm. They are shown in Fig. 1.

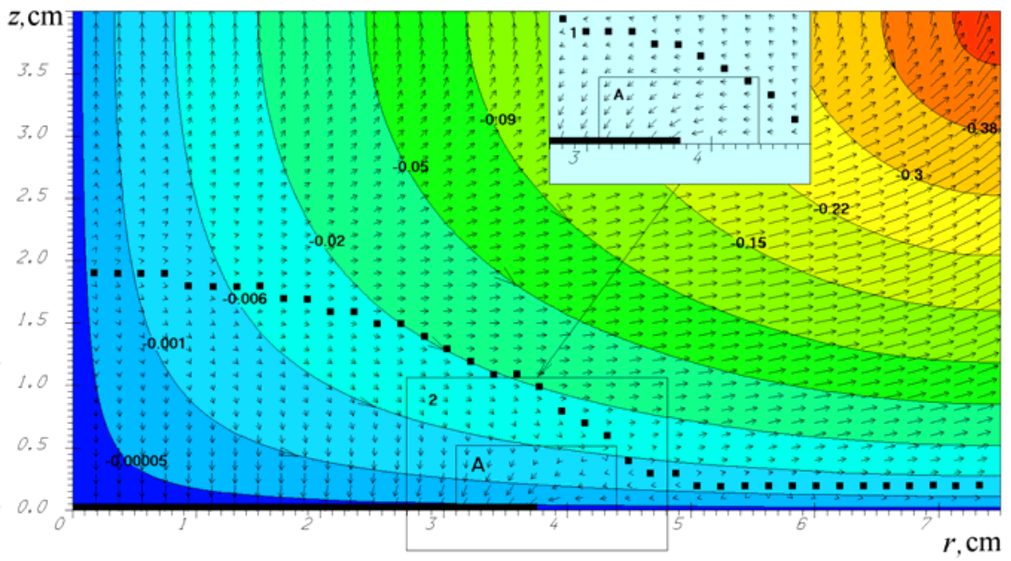


Fig. 2. Isolines of stream function and full flow of etchant reactant in "stadium" type reactor without the protector. 1, 2 - distributions of diffusion and full flows of etchant in zone **A**. Processing regimes: p = 0.2 torr, Q = 30 cm^3/min, I^+ = 0 mkA/cm^2.

The ends of cylinder chamber are employed as the electrodes between which the plasma RF-discharge is exited. The parent gas enters uniformly through upper electrode porous wall. The residual feed gas and products of dissociation, recombination and etching are pumped outwards either in radial ("stadium") or in axial ("pedestal") direction through circle gap on periphery of lower electrode.

It was noted that under operating in these industrial reactors an essential nonuniformity appeared at the outer edge of the patterns. As a consequence up to 30% of the initial wafer square went into a defective part. To minimize such an edge nonuniformity it was suggested to surround a pattern by a cylindrical protector with low etching reactivity. The problem was to obtain an optimal protector geometry.

For this purpose the dimensions and operating parameters were taken in the range which is characteristic for industrial reactors. The etching process of silicon Si in a tetrafluoromethane plasma CF_4 was chosen as a basic one. Because of relatively small temperature gradients during the etching process it was used the isothermal approach. In parametric calculations the multicomponent gas medium in a reactor was considered as binary gas mixture consisted of the fluorine atoms F supporting the etching reaction on the wafer and the feed gas CF_4. In this case the active species concentration distribution was derived by solving a single convection-diffusion equation with the generation term describing the generation (Eqs. (4), (5)) and depletion of active component in reactor volume (Eqs. (10), (11)).

To understand a mechanism of edge defect appearing and effect of protector the vector fields of fluorine flow densities were calculated:

$$\mathbf{Q}_e = \mathbf{Q}_c + \mathbf{Q}_d$$

where $\mathbf{Q}_e$ is the full flow density, $\mathbf{Q}_c = \mathbf{v}C_{\mathrm{F}}$ and $\mathbf{Q}_d = -D_{\mathrm{F}}C_t\nabla x_{\mathrm{F}}$ are the convective and diffusion ones correspondingly, D_{F} is the binary diffusivity of fluorine atoms in CF_4. The typical distribution of the full flow density $\mathbf{Q}_e$ in "stadium" reactor without protector is presented in Fig. 2.

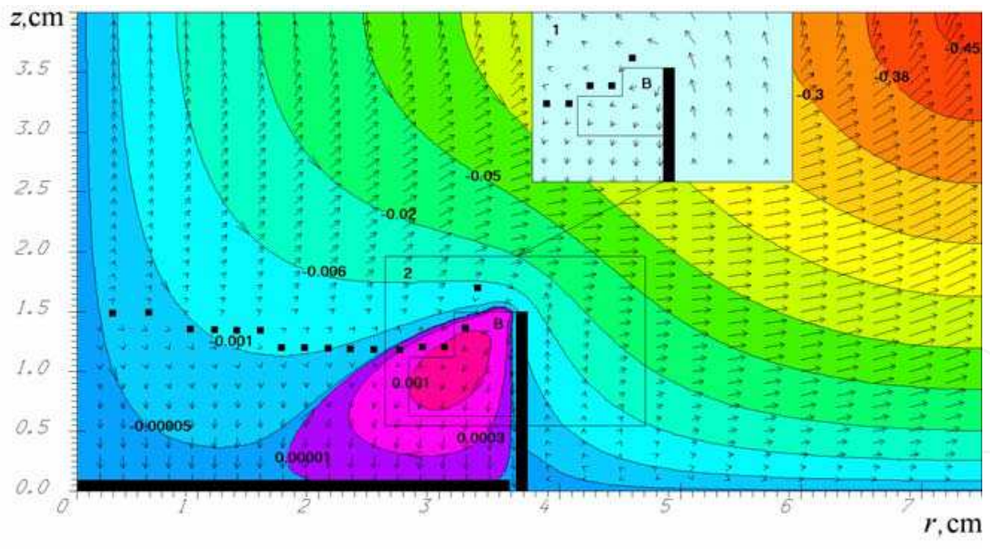


Fig. 3. The stream function isolines and distribution of full flow of etchant in "stadium" type reactor with optimal protector r_p = 38 mm, h_p = 15 mm. 1, 2 - distributions of diffusion and full flows of etchant in zone **B**. Processing regime: p = 0.2 torr, Q = 30 cm^3/min, I^+ = 0 mkA/cm^2.

One can see that near the outer edge the characteristic zone **A** exists where the relatively intensive diffusion of fluorine to the wafer takes place. It is connected with the large difference in etching reactivities of wafer and anode surfaces. The black markers single out

the layer where $\partial x_F / \partial z = 0$ and the diffusion flow changes a sign. Consequently the etching nonuniformity in this case is defined by the nonuniformity of diffusion flow near the wafer edge.

The parametric calculations for different values of height and diameter of a protector were fulfilled. The results allowed us to choose the optimal sizes of protector. Fig. 3 presents the full flows in "stadium" reactor with optimal protector. Thereat material of protector has a low reactivity. One can see from Fig. 3, that circle protector which has the same radius as the wafer interrupts completely the local diffusion flow arising from difference in reactivities of wafer and anode. Although near the top edge of protector zone **B** is appeared where the influence of low anode reactivity is preserved.

Despite of these results, obtained for the very simple plasma chemical kinetics, the further investigations have shown that the optimal protector provides high etching uniformity for enough complicated models also.

3.2 Heat radiation transfer and thermodiffusion

Plasma - chemical etching is usually related to the category of low temperature processes. Therefore, at the mathematical simulation of etching reactors one can limit himself by isothermal approach giving often the satisfactory results (Grigoryev & Gorobchuk, 1996). However the employment of low heatproof resists and thermosensitive polymers for the wafers requires thorough investigation of the heating the processing chip and the elements of reactor construction. Also it is necessary to determine the heating influence on the processing quality. The main sources of heating effects in reactor are the heat generation on the wafer and surrounded electrode by the energetic ion bombardment, plasma radiation, heat effects of the exothermic reactions and glow discharge. The heat removal is realized by the complex heat transfer in reactor chamber and by the cooling system if such a system exists. Some nonisothermal effects in the reactor as a function of the electrode and wafer temperature were investigated. The temperature was specified and varied in characteristic limits T_{w2} = 300 – 500 K (Grigoryev & Gorobchuk, 1997; Grigoryev & Gorobchuk, 1998). The heat radiation transfer in the gas was determined using the optical thin layer approximation. According to such an approach the source of heat radiation in (3) have the following form:

$$\nabla \cdot \mathbf{q}_r = -2\sigma\left[\kappa_p(T_{w1})T_{w1}^4 - \kappa_p(T)T^4 + \kappa_p(T_{w2})T_{w2}^4\right],$$

where κ_p is the Plank average absorption coefficient in the parent gas, σ is the Stefan-Boltzmann constant, T_{w1} is the temperature of cathode, T_{w2} is the temperature of anode. The problem which we have obtained consisted in the absence of the necessary data about the emissivity of CF_4. Because the value κ_p was estimated by the emissivity of methane CH_4 having the same structure and the similar main vibration modes as the molecule CF_4. For calculation of the spectral absorption coefficient κ_ν the exponential model of spectral band was used (Edwards & Menard, 1964). The boundary conditions on the temperature described the balance of heat flows, namely convective, heat conductive and radiative ones. For example, at the wafer surface:

$$-\lambda\frac{\partial T}{\partial z} = \alpha(T_{w2} - T) + \sigma\varepsilon\varepsilon_w(T_{w2}^4 - T^4), \quad 0 \le r \le r_1, z = 0,$$

where α is the heat transfer coefficient, ε_w is the emissivity of the wafer, ε is the emissivity of the gas.

The boundary conditions for fluorine species took into account the diffusion and thermodiffusion of active species, its heterogeneous recombination and consumption in the chemical reactions of spontaneous and ion - induced etching. For instance, the boundary conditions at the wafer surface had the following form (in binary approach):

$$D_{\mathrm{F}}\left(\frac{\partial x_{\mathrm{F}}}{\partial \mathrm{z}}+k_T\frac{\partial \ln T}{\partial z}\right)=k_s x_{\mathrm{F}}(1-\mu x_{\mathrm{F}})+k_i I^{+}(1-\mu x_{\mathrm{F}})/C_t,$$

$$\mu=1-m_F/m_{CF_4},\quad 0\le r\le r_1, z=0,$$

where k_T is the thermodiffusion ratio; k_s, k_i are the constants of spontaneous (Eq.(29)) and ion - induced etching (Eq.(30)); m_F, m_{CF_4} are the molecular masses of active species and parent gas, respectively.

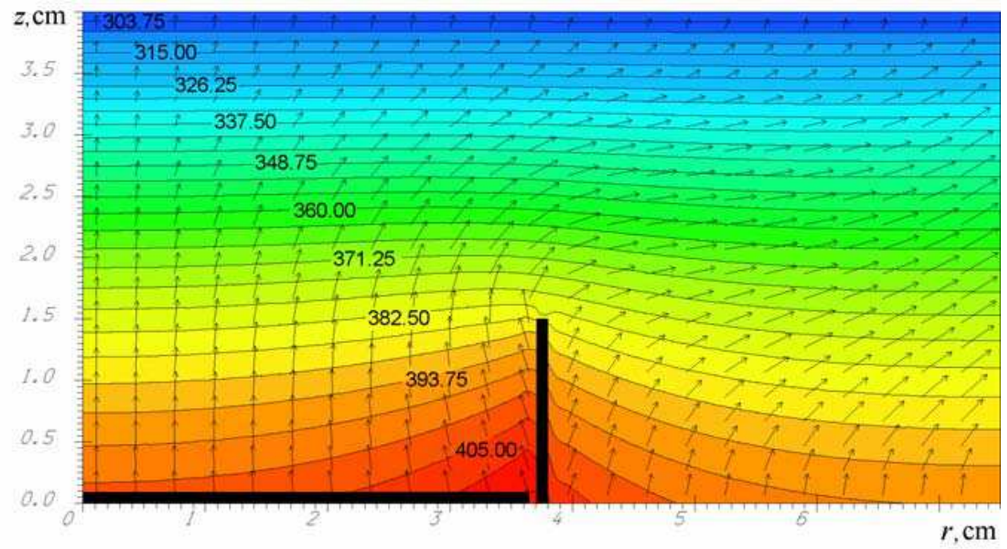


Fig. 4. The distribution of isotherms and full heat flow $\mathbf{q}_h$ in "stadium" type reactor. Processing regime: p = 1.0 torr, Q = 50 cm³/min, T_{w2} = 500 K, I+ = 0 mkA/cm².

In calculations the vector fields of local density heat flow were analyzed. It is consisted of three components:

$$\mathbf{q}_h=\mathbf{q}_a+\mathbf{q}_c+\mathbf{q}_r,$$

where

$$\mathbf{q}_a=\rho c_p T\mathbf{v},\quad \mathbf{q}_c=-\lambda\nabla T$$

are the densities of heat convective and heat conductive flows. The characteristic picture of full heat flow $\mathbf{q}_h$ distribution is shown in Fig. 4. It was obtained that the main contribution in $\mathbf{q}_h$ is given by the heat conduction and heat radiation flows in cylindrical volume over the substrate. In particular, near the wafer $|\mathbf{q}_c|\approx|\mathbf{q}_r|$, and they exceed convective flow $\mathbf{q}_a$ over two order. Simultaneously $\mathbf{q}_c$ and $\mathbf{q}_r$ have the same order at the outlet in the middle part of reactor, but $\mathbf{q}_a$ exceeds them by factor of 1.5 - 2. It is worth to note that if the heat radiation transfer is not taken into consideration the values of temperature on the isolines in Fig. 4 reduce approximately on 60K. This allows one to conclude that despite of the

temperature nonuniformities characteristic for etching reactors are relatively not large, the main heat transfer in the reactor realizes by the heat conduction and radiation. Therefore, a radiation heat transfer is necessary to take into account in numerical modelling.
Under the thermal nonuniformity conditions the flow density of active species may be written as follows:

$$\mathbf{Q}_e = \mathbf{Q}_c + \mathbf{Q}_d + \mathbf{Q}_t$$

where there are the convective flow $\mathbf{Q}_c = \mathbf{v}C_{\mathrm{F}}$, diffusion one $\mathbf{Q}_d \sim -D_{\mathrm{F}}\nabla x_{\mathrm{F}}$ and thermodiffusion one $\mathbf{Q}_d \sim -D_{\mathrm{F}}k_t\nabla \ln T$. The distribution of full flows $\mathbf{Q}_e$ of etchant is shown in Fig. 5.

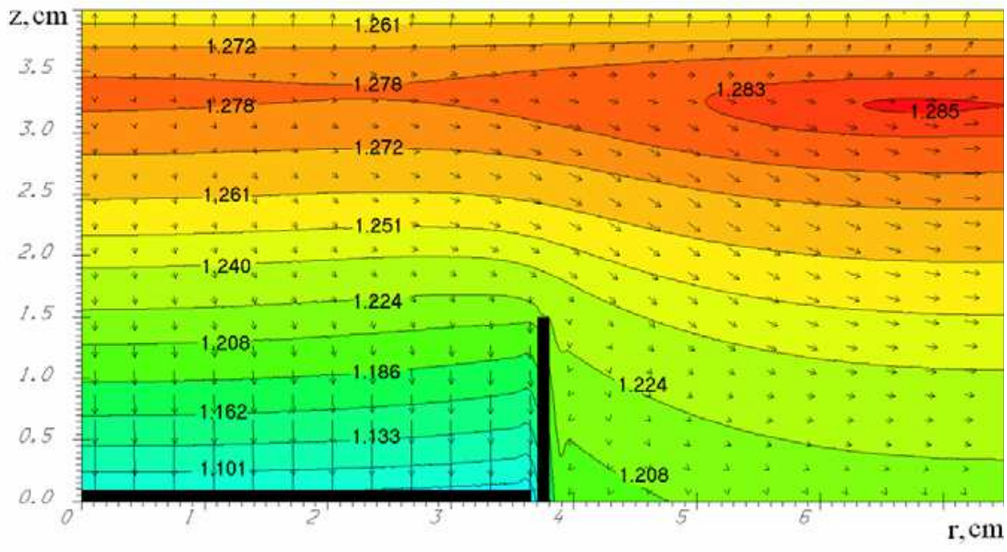


Fig. 5. The distribution of full flow of active species $\mathbf{Q}_e$ in "stadium" type reactor and isolines of concentration (C x 10^{-10}, mol/cm^3). Processing regime: p = 0.2 torr, Q = 50 cm^3/min, T_{w2} = 500 K, I^+ = 0 mkA/cm^2.

Since the thermodiffusion ratio $k_T < 0$, the vectors $\mathbf{Q}_t$ direct along the gradients of temperature. The calculations show that $|\mathbf{Q}_d| \approx |\mathbf{Q}_t|$ at the temperatures of lower electrode T_{w2} = 400 – 500 K outside of zone limited by the protector, and they determine the value of full flow $|\mathbf{Q}_d| \approx |\mathbf{Q}_t|$ substantially exceeding $|\mathbf{Q}_c|$. However immediately on the substrate $|\mathbf{Q}_t| \approx (0.1 \div 0.2)|\mathbf{Q}_d|$. It means that the direct contribution of the thermodiffusion $\mathbf{Q}_t$ to the etching processes gives 10 - 20% and under the local temperature gradients it may negatively affect the etching uniformity.
These conclusions about the significant role of the heat radiation and thermodiffusion have a general character for typical conditions of plasma etching process that was supported by our calculations of other reactor schemes.

3.3 Effect of choice of plasma etching kinetics

In foregoing decade the process of plasma chemical etching of silicon in CF_4 was studied by many authors for different reactors and some variants of chemical kinetics. Unfortunately,

different original data, geometrical configurations of reactors, numerous additional assumptions did not allow one to compare obtained results for choosing an adequate kinetic model. To do such a choice we have carried out a series of calculations of radial flow etching reactor that is a necessary aggregate in VLSI industry. The results obtained in the frameworks of one numerical model give us reliable data for comparison of wide used variants of Si - CF_4 plasma kinetics with respect to etching rate (Shokin at al., 1999).

The scheme of radial flow plasma - chemical etching reactor is shown in Fig. 1. The feed gas enters the reacting chamber at the outer edge of lower electrode. RF - discharge is appeared between the electrodes. Products of physical - chemical reactions are pumped from outlet in the centre of lower electrode. The processing wafer is placed on the lower electrode. The dimensions of reactor were taken from (Dalvie at al., 1986).

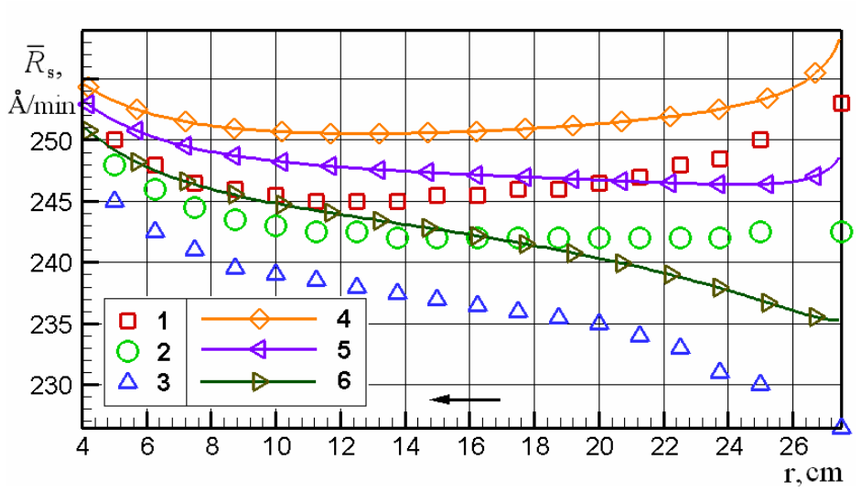


Fig. 6. Distributions of etching rate as a function of radial position along the wafer for different gas flow rate (inflow feed gas structure). Processing regimes: p = 0.525 torr, T_{w2} = 300 K. Designations: 1, 4 - Q = 300 cm³/min; 2, 5 - Q = 340 cm³/min; 3, 6 - Q = 400 cm³/min. Markers 1, 2, 3 - data of article (Dalvie at al., 1986). Markers 4, 5, 6 - author data.

The operating conditions of reactor and process parameters were varied in the range that is characteristic for industrial reactors. In particular, it was chosen: the pressure p = 0.5 torr, the gas flow rate Q = 300 – 400 cm³/min, the average electron density $\overline{n}_e$ =10^{10} cm^{-3}, the temperature of electrodes T_{w1} = 300 K, the temperature of wafer T_{w2} = 300 – 500 K. Since only a small fraction of tetrafluoromethane is dissociated under RF-discharge (<10%), all macroscopic characteristics of the medium - $\eta, \lambda, c_p, \kappa_p$ were chosen for the pure tetrafluoromethane CF_4. The dependencies of gas viscosity, thermal conductivity, heat capacity and absorption coefficient on the gas temperature and pressure were taken into account.

The homogeneous and heterogeneous reactions included in the basic kinetic model in these calculations was following: the reactions of fluorine production by electron - impact dissociation of parent gas Eqs. (4), (5); the reactions of volume recombination of reactive atoms and radicals Eqs. (9)-(11); the reactions of recombination of fluorine atoms, the recombination of CF_3 and the adsorption of CF_3 at wafer surface Eqs. (20), (23), (24); the reaction of silicon etching Eq. (29).

Before the comparison of kinetic models the test calculations with kinetics and data used in (Dalvie at al., 1986) have been fulfilled. At these conditions our simulations of isothermal reactor showed the satisfactory agreement with the results in (Dalvie at al., 1986). The comparison of the obtained profiles of etching rates with those reported in (Dalvie at al., 1986) are presented in Fig. 6.

The maximum relative and maximum root-mean-square errors did not exceed 0.05799 and 0.02166, correspondingly. Thus, it was shown that the results obtained by two different numerical methods coincide with a good accuracy. It allowed one to be sure in further results of comparison of the kinetic models.

A special interest of our research was a comparison of two-, three- and four- component kinetic models considered in (Grigoryev & Gorobchuk, 1996; Dalvie at al., 1986; Sang-Kyu Park & Economou, 1991) correspondingly. Two- and three-component kinetics were obtained as some simplifications of the basic kinetic model. Thereat it was essentially used that the concentrations of products of gas-phase reactions $C_{\mathrm{F}}, C_{\mathrm{CF}_2}, C_{\mathrm{CF}_3}$ are significantly smaller then the total gas concentration C_t and the unreacted feed gas concentration C_{CF_4}. For two-component kinetic model it was assumed that $C_{\mathrm{CF}_2} \sim C_{\mathrm{CF}_3} \sim C_{\mathrm{F}}$. In such a case only one component convection-diffusion equation was solved to calculate a fluorine concentration C_{F}. The concentrations $C_{\mathrm{CF}_2}, C_{\mathrm{CF}_3}$ were taken into account as parameters. Therefore, the net generation term in equation (31) describing the processes (9)-(11) introduced by some authors as follows:

$$G_{\mathrm{F}} = (k_{e1} + k_{e2})\overline{n}_e(1 - 3C_{\mathrm{F}}) - (k_{v2} + k_{v3})C_{\mathrm{F}}^2 \tag{32}$$

In (Edelson & Flamm, 1984; Plumb & Ryan, 1986) it was shown that the most important reactions are (4) and (9). The three-component kinetics incorporates two equations on F and CF_3 concentrations. The C_{CF_2} was regarded as the parameter ($C_{\mathrm{CF}_2} \sim C_{\mathrm{F}}$). Eventually the four-component kinetic model contains all above-mentioned equations for the species concentrations of F, CF_2, CF_3.

The spontaneous etching rate was calculated as follows:

$$R_s = 1.75 \cdot 10^{12}(1 - \vartheta_{\mathrm{CF}_3})C_{\mathrm{F}}T^{1/2}\exp\left[-\frac{E_e}{kT_{w2}}\right],$$

where R_s in Å/min; E_e = (0.108 ± 0.005) eV; T is the gas temperature near the wafer, K; ϑ_{CF_3} is the parameter of silicon coverage by CF_3. The average etching rate and fluorine concentration were determined by the formulas:

$$\overline{R}_s = \frac{2}{R_o^2 - R_i^2}\int_{R_i}^{R_o} R_s r dr, \qquad \overline{C}_F = \frac{2}{R_o^2 - R_i^2}\int_{R_i}^{R_o} C_F r dr, \qquad I_n = \frac{R_s^{\max} - R_s^{\min}}{2R_s}.$$

Their variation along the wafer as a function of temperature for two-, three- and four-component kinetics is presented in Table 1.

The obtained data show that the values of average etching rate and fluorine concentration obtained for two-, three- and four- component kinetic models are strongly differ from each other for any fixed reactor regime (see Table 1). These distinctions are connected with unsuccessful parametrization of species generation terms (32) in two- and three-component

models. The obtained results show that there is a problem of choosing of adequate kinetics for CF_4 - kinetics that up to day was not discussed in the corresponding studies. In order to solve this problem it is necessary to compare these results with the reliable experimental data. Unfortunately the latter are absent in the present-day existent literature.

T_{w2}, K	$\bar{R}_s$, Å/min			$\bar{C}_F \cdot 10^{-9}$, mol/cm^3			I_n		
	Number of components			Number of components			Number of components		
	2	3	4	2	3	4	2	3	4
Inflow									
300	83.05	373.50	624.94	0.17844	0.80833	1.34619	0.0888	0.1106	0.0528
373	189.17	823.89	968.95	0.16869	0.74013	0.86954	0.1017	0.1178	0.1049
473	389.56	1591.27	1377.89	0.15556	0.64741	0.56379	0.1168	0.1207	0.1513
573	608.61	2375.13	1707.10	0.14276	0.56176	0.40903	0.1286	0.1176	0.1846
Outflow									
300	83.02	373.30	599.01	0.17838	0.80789	1.29064	0.1762	0.2491	0.3009
373	189.10	823.48	930.54	0.16861	0.73966	0.83491	0.1943	0.2469	0.2869
473	385.09	1590.56	1314.05	0.15545	0.64704	0.53747	0.2156	0.2440	0.2982
573	607.99	2374.27	1610.66	0.14265	0.56168	0.38604	0.2340	0.2401	0.3088

Table 1. Average etching rate, average fluorine concentration and uniformity index: two-, three- and four- components kinetic models. Processing regime: p = 0.512 torr, Q = 340 cm^3/min.

3.4 Numerical optimization of silicon plasma etching in CF_4/O_2 mixture

The binary mixture CF_4/O_2 is a perspective parent gas for industrial plasma etching process that allows to increase essentially an etching rate of silicon wafers. Such mixtures are available commercially, but the number of papers devoted to mathematical modelling of this process are relatively small. Moreover in most studies the simplified models are used and the obtained results are inconsistent with experimental date in many effects. It is clear that the obtained numerical results depend on the choice of chemical kinetics and adequate modelling of complex heat-mass transfer.

In present calculations the improved chemical kinetic model (Venkatesan at al., 1990) was used including 12 all above mentioned components which are F, F_2, CF_2, CF_3, CF_4, C_2F_6, O, O_2, CO, CO_2, COF, COF_2. The heat-mass transfer in the reactor was calculated on the basis of two-dimensional mathematical model of nonisothermal reactor described above taking into account the chosen multicomponent chemical kinetics. The heat radiation in the gas mixture was determined in optical thin layer approximation. To evaluate the emissivity of gas mixture the exponential model of band adsorption (Edwards & Menard, 1964) describing the spectral adsorption of multiatomic molecules was employed.

Accordingly to existent representation of chemisorption process some parts of silicon surface are covered by various adsorbed atoms and radicals. Let $\vartheta_{CF_2}, \vartheta_{CF_3}$ are the fractions of silicon surface covered by adsorbed radicals CF_2 and CF_3 correspondingly; ϑ_O is the fraction of silicon surface covered by oxygen atoms, x_i is the molar fraction of i-th particles. Writing down the balance of mass flows for CF_2, CF_3 and O components on silicon surface at equilibrium as in (Venkatesan at al., 1990; Sang-Kyu Park & Economou, 1991) a system of linear equations for unknown parameters $\vartheta_{CF_2}, \vartheta_{CF_3}, \vartheta_O$ is obtained in the form:

$$\begin{cases} k_{s2}x_{CF_2} / (k_{s3}x_F + k_{s6}x_O) = \vartheta_{CF_2} / (1 - \vartheta_{CF_2} - \vartheta_{CF_3} - \vartheta_O) \\ k_{s1}x_{CF_3} / (k_{s4}x_F + k_{s5}x_{CF_3} + k_{s7}x_O) = \vartheta_{CF_3} / (1 - \vartheta_{CF_2} - \vartheta_{CF_3} - \vartheta_O) \\ \alpha_s x_O / x_F = \vartheta_O / (1 - \vartheta_{CF_2} - \vartheta_{CF_3}), \end{cases}$$

Solving this system allows to derive the next formulas for $\vartheta_{CF_2}, \vartheta_{CF_3}, \vartheta_O$:

$$\begin{aligned} \vartheta_{CF_2} &= k_{s2}x_{CF_2} / (k_{s2}x_{CF_2} + k_{s3}x_F + k_{s6}x_O + \Delta_{CF_2}), \\ \Delta_{CF_2} &= \Delta_{1,CF_2} + \Delta_{2,CF_2}, \\ \Delta_{1,CF_2} &= k_{s1}x_{CF_3}(k_{s3}x_F + k_{s6}x_O) / (k_{s4}x_F + k_{s5}x_{CF_3} + k_{s7}x_O), \\ \Delta_{2,CF_2} &= \alpha_s(k_{s3}x_F + k_{s6}x_O)x_O / x_F; \end{aligned}$$

$$\begin{aligned} \vartheta_{CF_3} &= k_{s1}x_{CF_3} / (k_{s1}x_{CF_3} + k_{s4}x_F + k_{s5}x_{CF_3} + \Delta_{CF_3}), \\ \Delta_{CF_3} &= k_{s7}x_O + \Delta_{1,CF_3} + \Delta_{2,CF_3}, \end{aligned} \tag{33}$$

$$\begin{aligned} \Delta_{1,CF_3} &= k_{s2}x_{CF_2}(k_{s4}x_F + k_{s5}x_{CF_3} + k_{s7}x_O) / (k_{s3}x_F + k_{s6}x_O), \\ \Delta_{2,CF_3} &= \alpha_s(k_{s4}x_F + k_{s5}x_{CF_3} + k_{s7}x_O)x_O / x_F; \end{aligned}$$

$$\vartheta_O = \alpha_s x_O / (\alpha_s x_O + x_F + \Delta_{1,O} + \Delta_{2,O}), \tag{34}$$

$$\begin{aligned} \Delta_{1,O} &= x_F k_{s2}x_{CF_2} / (k_{s3}x_F + k_{s6}x_O), \\ \Delta_{2,O} &= x_F k_{s1}x_{CF_3} / (k_{s4}x_F + k_{s5}x_{CF_3} + k_{s7}x_O), \end{aligned}$$

where the parameter $\alpha_s = k_{s8} / k_{s9}$ is introduced analogically with (Schoenborn at al., 1989; Kopalidis & Jorine, 1993). Such a presentation expresses these fractions through the rate constants of the processes.

A special case can be considered for ϑ_{CF_3} . By substitution to the Eq. (33) $x_{CF_2} = x_O = 0$ we derive the formula $\vartheta_{CF_3} \approx k_{s1}x_{CF_3} / ((k_{s1} + k_{s5})x_{CF_3} + k_{s4}x_F)$, which coincides with three component chemical kinetic model (Sang-Kyu Park & Economou, 1991).

In the second particular case supposing in formula Eq. (34) $x_F >> x_{CF_2}, x_{CF_3}$ one can carry out an expression

$$\vartheta_O \approx \alpha_s x_O / (\alpha_s x_O + x_F). \tag{35}$$

which coincides with formula for ϑ_O presented in (Kopalidis & Jorine, 1993). In this simplified expression the denominator reflects a competition of chemisorption processes of fluorine and oxygen atoms on silicon which leads to hysteresis effect on the diagram of etching rate with respect to fluorine concentration (Mogab at al., 1978).

Under assumption that $\vartheta_{CF_2}, \vartheta_{CF_3} << 1$ (Grigoryev & Gorobchuk, 2007), the parameter α_s in these formulas which contains unknown rate constants of Eqs. (27), (28) can be defined by the next ratio of fluorine and oxygen atoms adsorbed on the wafer:

$$\alpha_s \approx \frac{F_{\mathrm{O}} S_{\mathrm{O}}}{F_{\mathrm{F}} S_{\mathrm{F}}} = \frac{S_{\mathrm{O}}}{S_{\mathrm{F}}} \sqrt{\frac{m_{\mathrm{F}}}{m_{\mathrm{O}}}}, \quad F_j = \sqrt{\frac{kT}{2\pi m_j}}, \quad j = \mathrm{F,O}, \tag{36}$$

where m_j, F_j are the molecular mass and intensity of molecular flow of the j -th particles to the wafer; $S_{\mathrm{F}}, S_{\mathrm{O}}$ are the sticking coefficients of oxygen and fluorine atoms on silicon (Kopalidis & Jorine, 1993).

The parameter α_s indicates the intensity of oxygen chemisorption on silicon and essentially influence the location and amplitude of maximum etching rate (Grigoryev & Gorobchuk, 2007). The nonzero fraction ϑ_{O} leads to hysteresis effect on the diagram of etching rate versus the fluorine concentration.

Accordingly to an improved surface kinetic model which describes the competing processes of etching, chemisorption of O and adsorption of CF_2, CF_3 on silicon the local spontaneous etching rate in Å /min was defined by the formula:

$$R_s = 1.81 \cdot 10^{10} (1 - \vartheta_{\mathrm{O}} - \vartheta_{\mathrm{CF_2}} - \vartheta_{\mathrm{CF_3}}) k_s x_{\mathrm{F}} C_t,$$

where k_s is the etching rate constant, cm/s; C_t is the molar concentration of gas mixture, Mol/cm^3.

The radial flow reactor was considered in the calculations (see Fig. 1). The constructive dimensions and operating regimes were taken from (Venkatesan at al., 1990). The calculations have been done for several values of gas flow rate under normal conditions Q = 100, 200, 400, 800 cm^3/min. The wafer temperatures T_{w2} = 300, 373, 473, 573 K were considered. The pressure in etching chamber of reactor was equal to p = 0.5 torr. The average electron density was assumed equal to $\bar{n}_e$ = 6 x 10^9 cm^{-3}. The temperature of reactor walls was T_{w1} = 300 K. The O_2 percentage fraction in CF_4/O_2 feed gas mixture varied in the range 10-90%. Two gas flow directions were examined: "inflow", when the gas flow was directed to the centre of reactor, and "outflow" - with the reversed direction. It was of interest to study a distribution of fluorine flows and spontaneous etching rate in dependence on O_2 percentage fraction in feed mixture.

The distribution of fluorine flow in the reactor depends on many factors: operating regime of reactor, gas composition, direction of feed gas flow and etc. Figures 7-10 illustrates the distribution of flow structure, temperature, concentration and full flow of active species for outflow feed gas structure. The direction of fluorine mass transfer in the middle part of reactor height, where $|\mathbf{v}| >> w_0$, coincides with the direction of gas flow. Near the RF-electrodes, where the velocity of gas flow is small, the fluorine mass transfer is realized by a concentration diffusion. Owing to the intensive forced convection the nonuniform distribution of full flow of active species on the wafer is arisen. Because of that the full flow of active species deviates from the normal to the wafer. Finally, as one can see from Figure 10, the mass transfer of fluorine atoms to the wafer surface depends strongly on the convective transfer that confirms the known representations about process in a radial flow reactor.

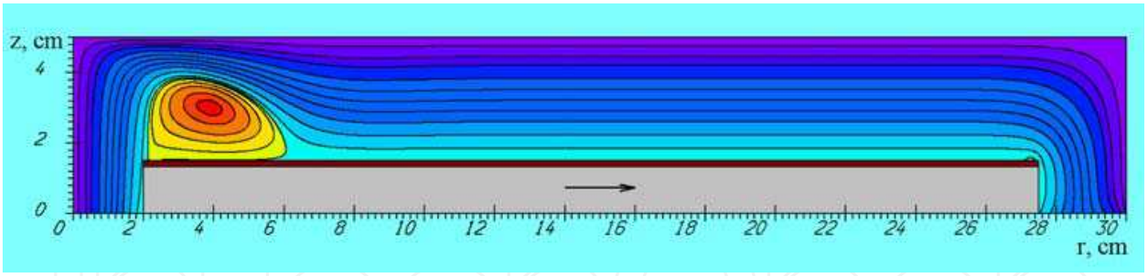


Fig. 7. The flow gas structure.
Processing regime: p = 0.5 torr, Q = 800 cm³/min, T_{w2} = 300 K, 30% fraction O_2 in CF_4/O_2.

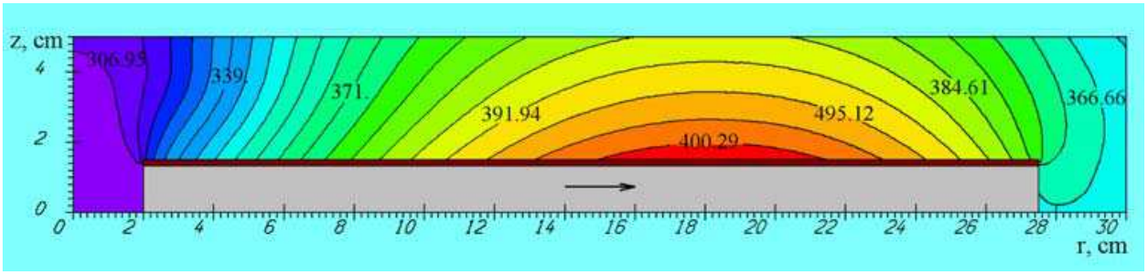


Fig. 8. The temperature distribution.
Processing regime: p = 0.5 torr, Q = 200 cm³/min, T_{w2} = 473 K, 30% fraction O_2 in CF_4/O_2.

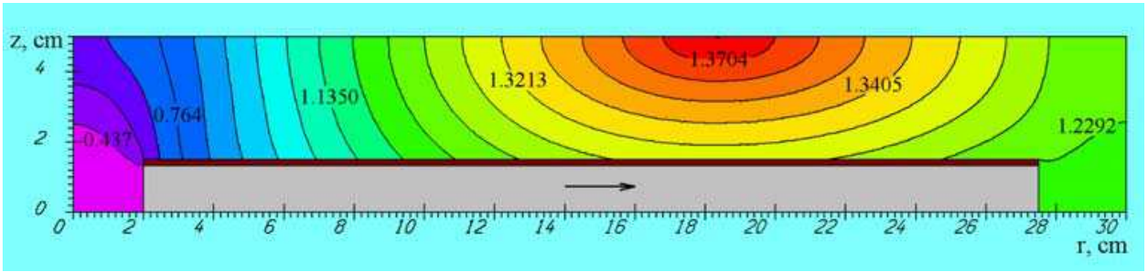


Fig. 9. The fluorine concentration distribution.
Processing regime: p = 0.5 torr, Q = 200 cm³/min, T_{w2} = 300 K, 40% fraction O_2 in CF_4/O_2.

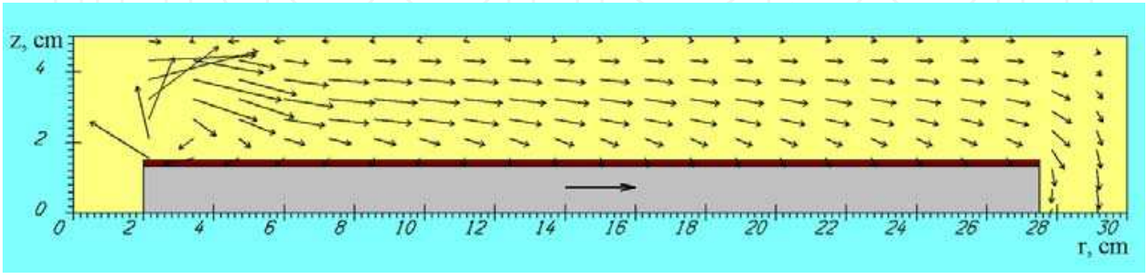


Fig. 10. The distribution of full flow of fluorine.
Processing regime: p = 0.5 torr, Q = 200 cm³/min, T_{w2} = 300 K, 40% fraction O_2 in CF_4/O_2.

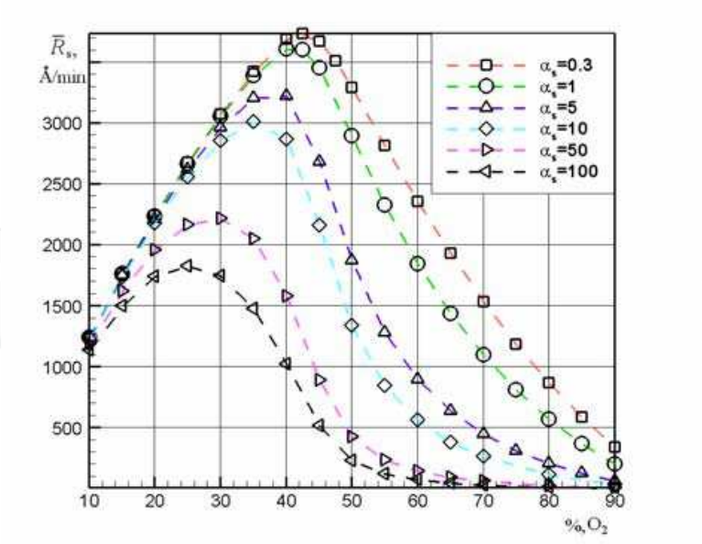


Fig. 11. Average etching rate as a function of percentage fraction of O_2 in CF_4/O_2 input mixture. Processing regime: p = 0.5 torr, Q = 200 cm^3/min, T_{w2} = 300 K. Case of "inflow" direction.

The sticking coefficients of oxygen and fluorine atoms on silicon are defined as in (Kopalidis & Jorine, 1993) S_F = 0.7, S_O = 0.2 which correspond to α_s = 0.3. In (Schoenborn at al., 1989) the chemical model included the similar parameter which was varied in the range 1 - 600. In our opinion such a range is too large, because it is clear the rise of α_s corresponds to increasing of ratio of sticking coefficients (Eq. (36)). Thereat in calculations the following values were examined α_s = 0.3, 1, 5, 10, 50, 100.

It was obtained that the average etching rate dependence on percentage fraction of O_2 in parent gas mixture has the maximum value about 40% of O_2. It takes place in the range of gas flow rate 100-400 cm^3/min (see Fig. 11, curve α_s = 0.3). In this case the maximum value of etching rate exceeds one's value in pure CF_4 more than in three times. With increasing of the gas flow rate up to 800 cm^3/min the maximum of etching rate moves to 30% of O_2. The location of extremum is independent of the feed gas flow direction and the gas temperature. With increasing O_2 percentage in gas mixture the fluorine concentration rises and has the maximum at 40% O_2. The decrease of CF_2, CF_3, CF_4, COF concentrations accompanies by the growth of fluorine concentration. The substances F_2, CO, CO_2, COF_2 are formed as the products of reactions. It corresponds to the one of channels of etching intensification by oxygen addition, which consists in the replacement of fluorine by oxygen in fluorine-containing radicals. With oxygen fraction more than 40% the fluorine concentration falls owing to decrease of the total number of CF_2, CF_3 radicals (depletion of mixture). Thus, the calculations show that the presence of etching rate maximum is connected with chemical reactions of oxygen atoms with CF_2, CF_3 radicals where the additional fluorine atoms are set free.

The etching rate dependence on fluorine concentration with different fractions of O_2 in CF_4/O_2 mixture obtained in calculations has a hysteresis character (see Fig. 12). Due to the passivation of wafer surface by oxygen atoms (with increasing ϑ_O) in the range of O_2 concentration more then 40% the silicon etching rate falls more quickly then fluorine

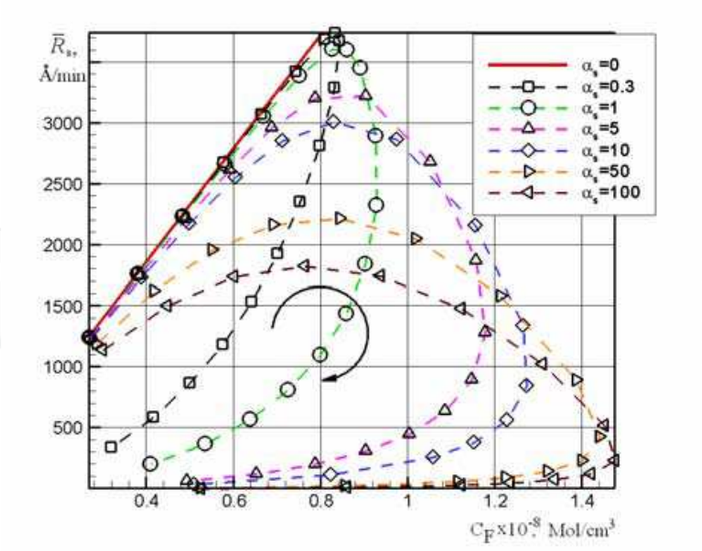


Fig. 12. Average etching rate as a function of average fluorine concentration on a wafer with different fractions of O_2 in CF_4/O_2 mixture. Processing regime: p = 0.5 torr, Q = 200 cm^3/min, T_{w2} = 300 K, "inflow" direction. The markers on the curves indicates O_2 fraction in CF_4/O_2 mixture varied in the direction of the arrow from 10% to 90% with 5% steps.

concentration. At the same time the hysteresis is not observed under the absence of oxygen chemisorption. It is illustrated by the linear dependence in Fig. 12 obtained for α_s = 0 and any fraction of O_2 in mixture. In this case the maxima of etching rate and fluorine concentration were achieved simultaneously at the same concentration of O_2 in CF_4/O_2 mixture that contradicted to experimental data (Mogab at al., 1978).

The parameter α_s essentially influence location and amplitude of maximum etching rate. With increase of parameter from 0.3 up to 100 the maximum of average etching rate moves from 40% fraction of O_2 in CF_4/O_2 to 25% (Fig. 11). At the same time the maximum of average fluorine concentration on Si surface is located near 50% fraction of O_2. The maximum value of etching rate decreases approximately in two time. This fact is connected with the passivation of Si surface by oxygen atoms (Eq. (27)) which prevents the reaction of fluorine with silicon (Eq. (29)). On the contrary because the etching rate decreases the maximum value of fluorine concentration two-fold rises. It is explained by additional yield of fluorine atoms which cannot use in the etching reaction owing to the surface passivation. The deviation between the maxima of normalized etching rate and normalized fluorine concentration at α_s = 0.3 was less than 3% of O_2 in the feed gas. This is inconsistent with experimental data where more large difference was observed. But this difference rises gradually with α_s and it arrives in the range 10 - 15% of O_2 at α_s = 1. This is agree with the real experimental data (Mogab at al., 1978) although the operating regimes of reactor and its dimensions were slightly different from using in the present work. This also means that limiting case for ϑ_O (Eq. (35)) describes an essential contribution in competition process. Probably a close sticking coefficients of oxygen and fluorine atoms when $\alpha_s \approx 1$ corresponds more realistic scenario of etching process. The displacement of maxima also affects on dependence of etching rate versus fluorine concentration (Fig.12). One can see from Fig.12 that with the rise of α_s the local maximum of etching rate shifts and becomes more lower

with simultaneous increasing maximal fluorine concentration. As a result the hysteresis curves become more circular. At the same time the beginning of curling of curve is gradually shifts to the region with small edition of O_2.

Generally these obtained results using complex kinetic model confirm the known experimental facts and qualitative scenario of silicon etching in CF_4/O_2 gas mixture. Particularly, the hysteresis effect is correctly reproduced. The oxygen addition up to 30 - 40% allows to increase the etching rate in several times and it is an effective factor for controlling the processing regime. The main channel of intensification of silicon etching in CF_4/O_2 gas mixture connects with a replacement of fluorine in CF_x radicals by oxygen atoms which set free the additional fluorine. The fluorine and oxygen chemisorption on silicon leads to hysteresis on the diagram of etching rate with respect to fluorine concentration. The influence of CF_2, CF_3 adsorption layers on the etching rate composes less 1% of nominal value. The variation of sticking coefficients of oxygen and fluorine atoms essential influence etching rate and hysteresis curve. With increase of its ratio α_s the maximum of average etching rate moves to the region with small edition of O_2. Thus, we have verified the very complex model of plasma etching reactor and have shown its opportunities.

3.5 Electron density effect on etching rate in plasma-chemical reactor

Electrical RF-discharges in fluorocarbon mixtures have been strongly studied for their effective employment in the production of semiconductor devices. Owing to different additions to the parent gas a variation of electron and ion concentrations in RF discharge may essentially affects on the main characteristics of etching process. In the case of Si - CF_4/O_2 system widely used in semiconductor production the addition of oxygen increases the spontaneous etching rate in several times and is an effective means for control of etching process as was shown above (see also experiments of Mogab at al., 1978). But at the same time the oxygen addition to tetrafluoromethane has a negative influence. According to the data of spectroscopic measurements (Mogab at al., 1978; Coburn & Chen, 1980; d'Agostino at al., 1980) the silicon etching process in CF_4/O_2 mixture accompanies by the electron concentration decrease with growing oxygen fraction when RF power and gas pressure being constants. This results in essential decrease of active particles generation at large oxygen contents. Further investigations (Coburn & Chen, 1980; d'Agostino at al., 1980) was shown that the influence of oxygen addition to CF_4 on electron density in RF-discharge is independent of construction dimensions of reacting chamber, operating regimes, electron energy (at least in the range 8-20eV) and has universal character.

Thus, the oxygen addition to CF_4 causes the contrary processes: on the one hand - the fluorine active particles production rises with simultaneously depletion of mixture by CF_x radicals. On the other hand - formation of oxygen chemisorption layer on silicon, decrease of electron concentration and dissociation efficiency of parent gas mixture also take place due to O_2 presence. Before our work the effect of electron concentration decrease in CF_4/O_2 mixture was not practically considered on the base of mathematical simulation.

The numerical results obtained illustrate an electron density influence on the main characteristics of silicon etching in dependence on oxygen concentration. In calculations it is compared the plasma-chemical reactors with uniform electron density distributions without oxygen $\overline{n}_e^0$ with $\overline{n} = \overline{n}_e^0 \times \vartheta(x_{O_2})$, where $\vartheta(x_{O_2})$ - the experimental dependence of average electron density on O_2 content (Mogab at al., 1978).

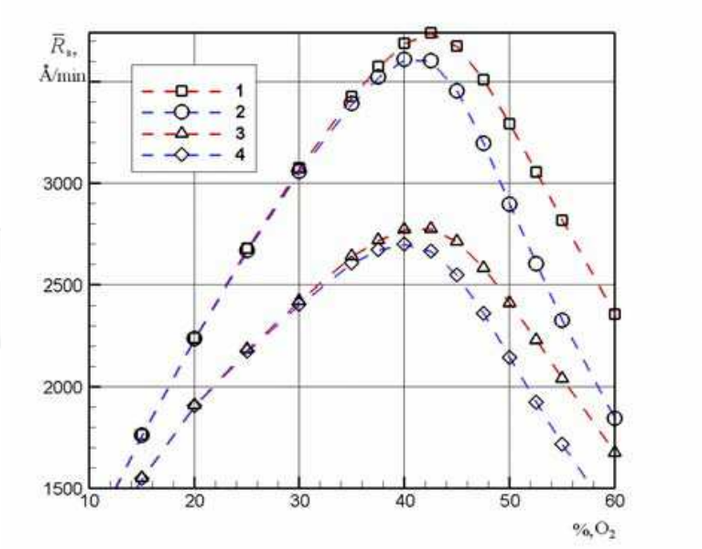


Fig. 13. Average etching rate vs percentage of O_2 in CF_4/O_2 mixture. Processing regime: p = 0.5 torr, Q = 200 cm^3/min, T_{w2} = 300 K, "Inflow" direction. Parameters: 1 – $\vartheta_e = 1$, $\alpha_s = 0.3$; 2 – $\vartheta_e = 1$, $\alpha_s = 1$; 3 – $\vartheta_e = \vartheta_e(x_{O_2})$, $\alpha_s = 0.3$; 4 – $\vartheta_e = \vartheta_e(x_{O_2})$, $\alpha_s = 1$.

The oxygen addition allows to increase essentially the concentration of active particles and etching rate of silicon wafers. The dependence of average spontaneous etching rate on the percentage of O_2 concentration in CF_4/O_2 illustrates this ability (see Fig. 13, curves 1, 2). At the same time the electron concentration monotonically falls down with the rise oxygen addition to CF_4 under other constant conditions. This decreases electron impact dissociation and ionization rates and leads to the reduction of active particle production. Simultaneously the average etching rate goes down (see Fig. 13, curves 3, 4). On can see from this diagrams that the visible separation of curves begins in the region of maximum etching rates at the oxygen concentrations more then 30%.

For characteristic of decrease of average etching rate and dissociation efficiency of parent gas mixture the relative deviations were calculated:

$$\delta_{\overline{R}_s} = \left| \frac{\overline{R}'_s - \overline{R}''_s}{\overline{R}'_s} \right|, \delta_{\overline{C}_i} = \left| \frac{\overline{C}'_i - \overline{C}''_i}{\overline{C}'_i} \right|, i = \mathrm{F}, \mathrm{CF_4}, \mathrm{O_2}.$$

Here $\overline{R}'_s$, $\overline{C}'_i$ are the average etching rate and fluorine, tetrafluoromethane and oxygen concentrations correspondingly at $\vartheta_e = 1$; $\overline{R}''_s$, $\overline{C}''_i$ are the average values with taking into account the dependence $\vartheta_e(x_{O_2})$.

Due to O_2 addition under other constant conditions an electron density monotonous decreases that causes the fall of fluorine concentration and etching rate. With the rise of percentage of O_2 content in CF_4/O_2 in the limits up to 60% the decrease of average etching rate can reach 30%. The quantitative deviations of average fluorine concentration at the wafer in the limits 0-40% O_2 addition coincide with the deviations of average etching rate. The last shows that in the limits etching rate dependence on fluorine concentration is practically linear and adsorption of CF_2, CF_3 particles on the wafer is weak. With taking into

account the dependence $\vartheta_e(x_{O_2})$ there are no qualitative differences in the average etching rate and fluorine concentration distributions as functions of O_2 addition. The location of the average etching rate maximum is preserved and is defined only by the intensity of oxygen chemisorption on silicon (parameter α_s) (Grigoryev & Gorobchuk, 2007). With increasing α_s the relative deviations of etching rate due to lowering electron density are preserved.

%, O_2	%, $\delta_{\bar{R}_s}$	%, $\delta_{\bar{C}_F}$	%, $\delta_{\bar{C}_{CF_4}}$	%, $\delta_{\bar{C}_{O_2}}$
10	8.95	8.95	2.05	25.98
20	14.79	14.74	8.41	42.07
30	21.22	21.07	22.25	58.75
40	24.88	24.44	44.15	66.49
50	26.66	26.86	68.82	74.99
60	28.90	29.66	81.61	84.58

Table 2. The values of $\delta_{\bar{R}_s}$, $\delta_{\bar{C}_F}$, $\delta_{\bar{C}_{CF_4}}$, $\delta_{\bar{C}_{O_2}}$ in dependence on O_2 addition.

The calculations of silicon etching process in CF_4/O_2 plasma including the experimental data on electron density decrease with oxygen addition allow to formulate the following conclusions. The fall of electron density in a RF-discharge with O_2 addition may decrease a spontaneous etching rate in the range up to 30%. At that the decrease in the range close to optimal etching rates arrived at 25 - 40% O_2 addition exceed 20%. Nevertheless the main positive effect of O_2 addition on the rise of etching rate in CF_4/O_2 mixture as compared with pure tetrafluoromethane preserves.

4. Some further perspectives

The perspectives of applications of created modelling tools in working up of new reactor schemes in the framework of silicon technology are obvious. Traditionally the parametric calculations will help design engineers in choosing the optimal configuration and operating parameters of the reactor.

The new technical challenges will require to model some new processes. For example, in present time the industry moves to production of largest single wafers with diameters up to 12 or even 16 inches (Japanese program). Under processing such large patterns the thermal and gravitational stresses will pose a strong limitation on the maximum wafer temperature and maximum temperature gradients near the wafer surface. This new problem will demand a very precise account of all wafer heating effects such as energetic ion bombardment, plasma radiation, heat generation by the exothermic reactions and glow discharge. It will be necessary to model in detail the real cooling system calculating thoroughly a problem of complex conjugate heat transfer. Furthermore it is need to include in the consideration the problems of an elasticity and thermoelasticity of a semiconductor wafer.

Besides we would like to draw attention to a new direction in mathematical modelling of chip manufacturing. In nearest future the typical fabrication-line for making complex chips

will be characterized by high level of programming automation, high quality operations and high yields. The new generations of micro- and nano-devices will demand a permanent (so called *in situ*) monitoring and control by their manufacturing in a real time (Orlikovsky at al., 2001). Monitoring data are to be operated and introduced in control system to support the optimal characteristics of process.

The relatively simple control system is based on supporting some goal parameter (parameters) on the optimal level using the controller. In this case the controller compares the current values of the goal parameters measured by monitoring system with ones from *apriori* calculated response functions. The calculating of response functions is a new problem of mathematical modelling.

The etching rate R_s can be considered as the goal parameter depending on the variable parameters such as flow rate Q, discharge power P, parent gas composition, etc. The calculated response functions are approximated by interpolation formulas, for example, by 2-dimensional cubic splines:

$$z^{(k)} = \sum_{i,j=1}^{M,N} \sum_{0 \le m+n \le 3} a_{ij}^{(m,n)} (x^{(l)} - x_i^{(l)})^m (x^{(r)} - x_j^{(r)})^n, \quad k,l,r = 1,2,...$$

where $\left\{ z^{(k)} \right\}$ is the set of goal parameters, $\left\{ x^{(l)} \right\}$ are the sets of variable parameters. These formulas are written in operating storage of controller. The data on the actual values $\left\{ z^{(k)}(t) \right\}$ from *in situ* sensors are also transmitted there. The results of their comparison in the form of parameter disbalance $\Delta z^{(k)}(t) = z^{(k)}(t) - z^{(k)}$ are converted by the controller into the new set of optimizing variable parameters $\left\{ x^{(l)} \right\}$. For example, the action of known proportional-integral - differential controller (Orlikovsky at al., 2001) is described by the following equation:

$$x^{(l)} = K \left[\Delta z^{(k)}(t) + \frac{1}{T_i} \int \Delta z^{(k)}(t) dt + T_d \frac{d\Delta z^{(k)}(t)}{dt} \right] \quad l = 1,2,...$$

The executor installs the new set of variable parameters on a reactor.

The most impressive new project in mathematical modelling of glow reactors is a creation of a virtual plasma chemical reactor. It is a comprehensive computational model of reactor processes that in first turn sets aside for the real time control of manufacturing process in flexible automation system. Such a composition is presented on Fig. 14 (Orlikovsky at al., 2001).

It is supposed that the computational model of virtual reactor will be organized in modular principle. It must contain a module 1 for calculations of electromagnetic (E - M) fields. The fields are describe by Maxwell - Lorentz system with taking into account a plasma bulk charge.

In the module 2 according to the given fields the electron density n_e and the energy T_e are calculated. In particular, in this module the Boltzmann kinetic equation for electron energy density distribution function (DDF) can be solved. Let us note that such an approach is a very laborious method which restricts the possibility to work in a real time. But here one can use so called hydrodynamic approach.

In the module 3 the gas flow structure and the temperature field in the reactor are computed. The module 4 carries out the calculations of plasma chemical kinetics and

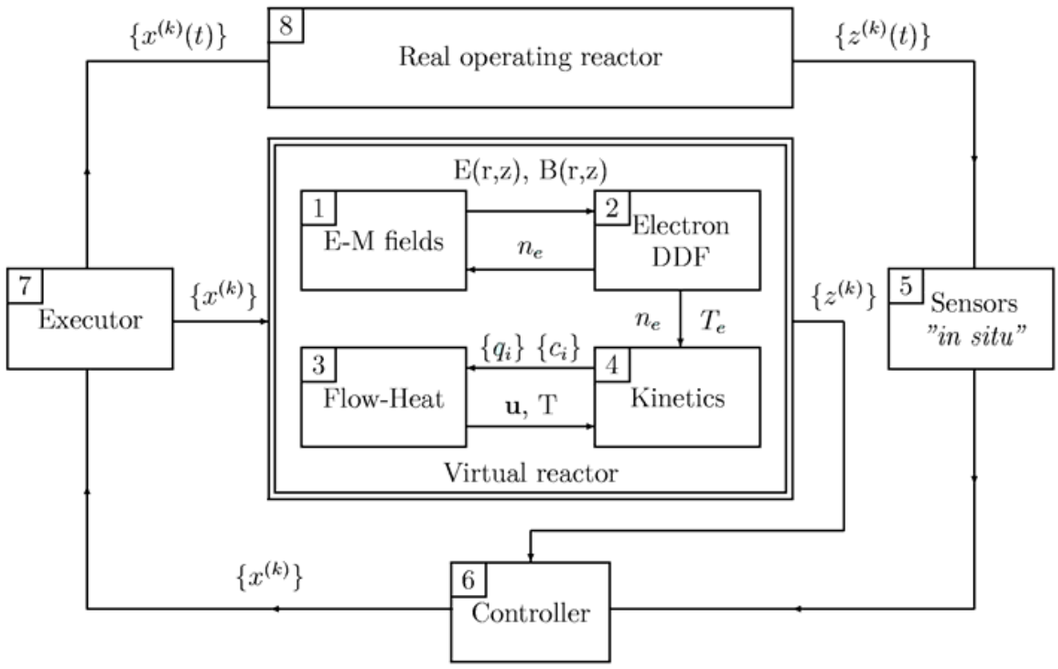


Fig. 14. Scheme of flexible automation system with virtual reactor

computes a mass transfer using of velocity and temperature fields. In turn, the data on gas component concentrations and thermal effects of chemical reactions are taken into account in the module 3. When using the virtual reactor in automation system the response functions $\left\{z^{(k)}\right\}$, calculated in real time with the actual process parameters, are transmitted in module 6 (controller). The data of *in situ* sensors $\left\{z^{(k)}(t)\right\}$, treated in the module 5, are also transmitted in this module. As it was said above the controller converts the results of their comparison in a set $\left\{x^{(l)}\right\}$ of optimizing variable parameters. The latest are simultaneously communicated both in the executor 7 and in the virtual reactor. In the virtual reactor the optimal goal parameters are calculated again. In such a way the feedback is closed.

As a comprehensive computational model of plasma chemical processing the virtual reactor can be used also by design engineers, in the calculations of more precise response functions for using in simple control systems described above, and as a learning automaton for personnel.

5. Acknowledgment

This research was supported by the Russian Fund of Fundamental Research (grant No.07-01-00315, No.08-01-00116) and RFOSS (grant No.931.2008.9).

6. References

Aydil, E.S. & Economou, D.J. (1993) Modelling of plasma etching reactors including wafer heating effects. *Journal of the electrochemical society*, Vol.140, No.5. pp.1471-1481.

Coburn, J.W. & Chen, M. (1980) Optical emission spectroscopy of reactive plasmas: A method for correlating emission intensities to reactive particle density. *Journal of applied physics,* Vol.51, pp.3134-3136.

d'Agostino, R., Cramarossa, F., De Benedicts, S. & Ferraro, G. (1980) Spectroscopic diagnostics of CF_4-O_2 plasmas during Si and SiO_2 etching processes. *Journal of applied physics*, Vol.52. No.3. pp.1259—1265.

Dalvie, M., Jensen, K.F. & Graves D.B. (1986) Modelling of reactors for plasma processing. I. Silicon etching by CF_4 in a radial flow reactor. *Chemical engineering science*, Vol.41, No.4. pp.653-660.

Edelson, D. & Flamm, D.L. (1984) Computer simulation of a CF_4 plasma etching of silicon. *Journal of applied physics*, Vol.56. pp.1522-1531.

Edwards, D.K. & Menard, W.A. (1964) Comparison of models for correlation of total band absorption. *Applied optics*, Vol.3, No.5. pp.621-625.

Grigoryev, Yu.N. & Gorobchuk, A.G. (1996) Numerical optimization of planar reactors of individual plasma-chemical etching. *Surface*, No.2, pp.47-63. (in Russian)

Grigoryev, Yn.N. & Gorobchuk, A.G. (1997) Numerical simulation of plasma-chemical etching reactors, *Proceedings of 21st International conference on microelectronics MIEL'97*, pp. 485-488, Nis, Yugoslavia, 14-17 September 1997.

Grigoryev, Yn.N. & Gorobchuk, A.G. (1998) Nonisothermal effects in plasma-chemical etching reactor. *Microelectronics*, Vol.27, No.4. pp.294-303. (in Russian)

Grigoryev, Yu.N. & Gorobchuk, A.G. (2004) Numerical modeling of silicon etching in CF_4/O_2 plasma-chemical system, *Proceedings of 24th International conference on microelectronics MIEL'2004*, pp.475-478, Nis, Serbia and Montenegro, 16-19 May 2004.

Grigoryev, Yn.N. & Gorobchuk, A.G. (2007) Specific features of intensification of silicon etching in CF_4/O_2 plasma. *Russian Microelectronics*, Vol.36, No.5. pp.368-379, ISSN 1063-7397.

Grigoryev, Yu.N., Gorobchuk, A.G. (2008) Effect on electron density in RF-discharge on etching rate in plasma-chemical reactor, *Proceedings of International conferencee 2008 IEEE Region 8 International Conference on "Computational Technologies in Electrical and Electronics Engineering" SIBIRCON 2008*, pp.322-327, Novosibirsk, Russia, July 21-25, 2008.

Kopalidis, P.M. & Jorine J. (1993) Modeling and experimental studies of a reactive ion etcher using SF_6/O_2 chemistry. *Journal of the electrochemical society*, Vol.140, No.10. pp.3037-3045.

Mogab, C.J., Adams, A.C. & Flamm, D.L. (1978) Plasma etching of Si and SiO_2 - The effect of oxygen additions to CF_4 plasmas. *Journal of applied physics*, Vol.49. No.7. pp.3796-3803.

Orlikovsky, A.A., Rudenko, K.V. & Suhanov, Ya.N. (2001) Diagnostics in situ of plasma technological processes of microelectronics: present-day state and nearest perspectives. Part IV. *Microelectronics*, Vol.30, No.6. pp.403-433. (in Russian)

Plumb, I.C., & Ryan, K.R. (1986) A model of the chemical processes occurring in CF_4/O_2 discharges used in plasma etching. *Plasma Chemistry and Plasma Processing*, Vol.6, No.3. pp.205-230.

Sang-Kyu Park & Economou, D.J. (1991) A mathematical model for etching of silicon using CF_4 in a radial flow plasma reactor. *Journal of the electrochemical society*, Vol.138, No.5. pp.1499-1508.

Schoenborn, Ph., Patrick, R. & Baltes H.P. (1989) Numerical simulation of a CF_4/O_2 plasma and correlation with spectroscopic and etch rate data. *Journal of the electrochemical society*, Vol.136, No.1. pp.199-205.

Shokin, Yu.I., Grigoryev, Yu.N. & Gorobchuk, A.G. (1999) Advanced optimization of etching processes in radial flow plasma-chemical reactor, *Proceedings of 8th International symposium on Computational Fluid Dynamics ISCFD'99*, Bremen, Germany, 5-10 September 1999, ZARM University of Bremen, Bremen.

Venkatesan, S.P., Trachtenberg, I. & Edgar, Th.F. (1990) Modelling of silicon etching in CF_4/O_2 and CF_4/H_2 plasmas. *Journal of the electrochemical society*, Vol.137, No.7. pp.2280-2290.

IntechOpen



Micro Electronic and Mechanical Systems

Edited by Kenichi Takahata

ISBN 978-953-307-027-8

Hard cover, 386 pages

Publisher InTech

Published online 01, December, 2009

Published in print edition December, 2009

This book discusses key aspects of MEMS technology areas, organized in twenty-seven chapters that present the latest research developments in micro electronic and mechanical systems. The book addresses a wide range of fundamental and practical issues related to MEMS, advanced metal-oxide-semiconductor (MOS) and complementary MOS (CMOS) devices, SoC technology, integrated circuit testing and verification, and other important topics in the field. Several chapters cover state-of-the-art microfabrication techniques and materials as enabling technologies for the microsystems. Reliability issues concerning both electronic and mechanical aspects of these devices and systems are also addressed in various chapters.

How to reference

In order to correctly reference this scholarly work, feel free to copy and paste the following:

Yurii N. Grigoryev and Aleksey G. Gorobchuk (2009). Numerical Simulation of Plasma-Chemical Processing Semiconductors, Micro Electronic and Mechanical Systems, Kenichi Takahata (Ed.), ISBN: 978-953-307-027-8, InTech, Available from: http://www.intechopen.com/books/micro-electronic-and-mechanical-systems/numerical-simulation-of-plasma-chemical-processing-semiconductors

INTECH
open science | open minds

InTech Europe
University Campus STeP Ri
Slavka Krautzeka 83/A
51000 Rijeka, Croatia
Phone: +385 (51) 770 447
Fax: +385 (51) 686 166
www.intechopen.com

InTech China
Unit 405, Office Block, Hotel Equatorial Shanghai
No.65, Yan An Road (West), Shanghai, 200040, China
中国上海市延安西路65号上海国际贵都大饭店办公楼405单元
Phone: +86-21-62489820
Fax: +86-21-62489821

© 2009 The Author(s). Licensee IntechOpen. This chapter is distributed under the terms of the Creative Commons Attribution-NonCommercial-ShareAlike-3.0 License, which permits use, distribution and reproduction for non-commercial purposes, provided the original is properly cited and derivative works building on this content are distributed under the same license.

IntechOpen

IntechOpen